Role of blocking ADAM10 hydrolysis site on N-cadherin by single-chain antibody in ventricular remodeling

XIAOOU LI[1*], WEI HUANG[2*], BING HE[1], LIRONG ZHOU[2], XIAOGANG HUANG[2] and BAOZHEN YAO[1]

[1]Department of Pediatrics, Renmin Hospital, Wuhan University, Wuhan, Hubei 430060; [2]Department of Preclinical Medicine, Wuhan Institute of Medical Sciences, Wuhan, Hubei 430014, P.R. China

Received September 14, 2016; Accepted June 2, 2017

DOI: 10.3892/etm.2017.5057

Abstract. The present study aimed to investigate the roles of the hydrolytic process of N-cadherin by A disintegrin and metalloproteases 10 (ADAM10) in sustaining myocardial structure and integrity, and discuss the mechanisms of ventricular remodeling in dilated cardiomyopathy (DCM). Single chain variable fragment antibody (ScFv) with the ability to specifically block the ADAM10 hydrolysis site of N-cadherin was designed and constructed. Western blot analysis and flow cytometry were used to detect the expression of N-cadherin and its C-terminal fragment 1 (CTF1) on cardiomyocytes, and cells were also subjected to a cell adhesion assay. Furthermore, in a rat model of dilated cardiomyopathy (DCM), the effects of intracardiac injection of the recombinant adenovirus on cardiac structure and contractile function were observed by hematoxylin and eosin staining and color Doppler echocardiography. The recombinant ScFv-expressing adenoviral plasmid with the ability to block the ADAM10 hydrolysis site on N-cadherin was successfully constructed and efficiently transfected into H9C2 cells. After transfection, N-cadherin protein expression was significantly increased, CTF1 protein was significantly decreased and the adhesion capability of myocardial cells was significantly improved. In the *in vivo* experiment, N-cadherin expression was significantly increased in the treatment group compared with that in the model group, and the structure and function of the heart were significantly improved. In conclusion, blocking of the ADAM10 hydrolysis site on N-cadherin by ScFv increased N-cadherin expression and improved ventricular remodeling. The present study provided experimental evidence for a novel approach for the treatment and prevention of DCM.

Correspondence to: Professor Baozhen Yao, Department of Pediatrics, Renmin Hospital, Wuhan University, 99 Zhang Zhi Dong Street, Wuchang, Wuhan, Hubei 430060, P.R. China
E-mail: professoryao@aliyun.com

Dr Wei Huang, Department of Preclinical Medicine, Wuhan Institute of Medical Sciences, 47 Li Huang Pi Road, Jangan, Wuhan, Hubei 430014, P.R. China
E-mail: huangwei_tj@aliyun.com

*Contributed equally

Key words: N-cadherin, ADAM10 hydrolysis site, dilated cardiomyopathy

Introduction

Dilated cardiomyopathy (DCM), which is one of reasons for heart failure, is a type of cardiac disease featuring enlargement of the heart chamber and dysfunction of the left or right ventricle and myocardial systole. At present, the prognosis of affected patients is poor and effective treatments are lacking (1). Studies have demonstrated that ventricular remodeling is a critical process of heart failure from compensation to decompensation and from reversible to irreversible, and that a key step for preventing the development of heart failure is to control the progression of ventricular remodeling (2-4).

The morphological characteristics associated with ventricular remodeling in DCM are ventricular dilation, a thinned ventricular wall and increased ventricular sphericity. At the cellular level, ventricular remodeling is characterized by the elongation and slippage of myocardial cells (5,6). It is well known that intercalated disks are the connecting structures to integrate myocardial cells into a whole tissue. The development of ventricular remodeling is closely associated with the abnormal structure and function of intercalated discs (7). N-type cadherin (N-cadherin) is an important medium among cells and matrix, which forms the N-type cadherin/catenin complex (cadherin-catenin complex) and functions as an important connection component. The cadherin-catenin complex is the molecular basis for the formation of intercalated disk structure to maintain the normal structure and function of the heart (8). Numerous studies have indicated that ventricular remodeling in DCM is closely associated with abnormal expression and distribution of the cadherin-catenin complex (9-11). In a hamster model of DCM, it was found that the expression of the cadherin-catenin complex in myocardial cells was significantly decreased, and the structure of intercalated discs was abnormal (12). After specific knockout of the N-cadherin gene in mature mice, no intercalated disks were present and similar ventricular remodeling to that in DCM was observed in these mice (13).

The normal functioning of the cadherin-catenin complex depends on its integrity, and abnormality of any

component affects the cell adhesion function mediated by N-cadherin (14,15). A disintegrin and metalloproteases (ADAMs) have an important role in the processing of N-cadherin in fibroblast and nerve cells (16). ADAMs hydrolyze N-cadherin at the R714-I715 site of the extracellular domain in the N-terminus, which then affects the cadherin-catenin complex, resulting in loss of function and corresponding pathophysiological changes, such as depressed neuronal cell adhesion and neurite outgrowth (16,17). It has been demonstrated that the normal function of the processing of N-cadherin by ADAMs is important in fibroblasts and nerve cells (16). ADAM9, -10 and -17 participate in the processing of N-cadherin, with ADAM10 having the most important role (18).

A previous study by our group found that ADAM10 had important roles in processing N-cadherin substrate in myocardial cells (19). Furthermore, ADAM10 expression was reported to be abnormally high in myocardial cells of DCM patients (20). In the present study, a single chain variable fragment antibody (ScFv) with the ability to specifically block the ADAM10 hydrolysis site on N-cadherin was designed and used to interfere with the hydrolysis of N-cadherin by ADAM10. The effect of ScFv on N-cadherin levels and ventricular remodeling was assessed.

Materials and methods

Synthesis of ScFv. According to the conserved sequence of the variable framework regions in the antibody-encoding gene, primers for amplification and splicing of the heavy chain variable domain (V_H) and light chain variable domain (V_L) were designed and synthesized by Invitrogen (Thermo Fisher Scientific, Inc., Waltham, MA, USA). The following primers were used: V_H upstream (P_{HA}), 5'-CAGGTSMARCTGCAG SAGTCWGG-3', downstream without linker sequence (P_{HB1}), 5'-TGAGGAGACGGTGACCGTGGTCC-3' and downstream containing linker sequence P_{HB}, 5'-GCCAGAGCCACCTCCG CCTGAACCGCCTCCACCTGAGGAGACGGTGACCGTG GTCC-3'; V_L downstream primer (P_{LC}), 5'-CCGTTTGATTTC CAGCTTGGTCCC-3', upstream without linker sequence (P_{LD1}), 5'-GACATCGAGCTCACCC AGTCTC-3' and upstream containing linker sequence (P_{LD}), 5'-CAGGCGGAG GTGGCTCTGGCGGTGGCGGATCGGA CATCGAGC TCACCCAGTCTC-3'. As it was not easy to amplify the V_H and V_L regions with primers containing the linker sequences, nucleotides without linker sequences (named V_{H1} and V_{L1}) were synthesized using the primers P_{HA}, P_{HB1}, P_{LC} and P_{LD1}. The purified V_H and V_L fragments were linked together to obtain ScFv by gene splicing through overlap extension polymerase chain reaction (SOE-PCR). Finally, ScFv was amplified using P_{HA}/P_{LC} primers with the SOE-PCR product as a template. Through Tag enzyme amplification, ScFv was linked into pMD-19T (both from Takara Biotechnology Co., Ltd., Dalian, China), and Sanger DNA sequencing technology (Thermo Fisher Scientific, Inc.) was used to identify successfully constructed pMD-19T-ScFv. The ScFv was amplified by PCR using pMD-19T-ScFv as a template, and the following primers were used: upstream primer (5'-ATAGGTACCGCC ACCATGCAGGTGCAACTGCAGGA-3' containing the *Kpn*I site, GGTACC) and downstream primer (5'-GGCAAGCTT TTAGTTTGATTTCCAGC TTGGTC-3 containing the *Hin*dIII site, AAGCTT). Taq DNA polymerase was purchased from Takara Biotechnology Co., Ltd. The PCR reaction program started with 5 min at 94˚C, which was followed by 30 cycles of 30 sec at 94˚C, 30 sec at 56˚C and 1 min at 72˚C, and a final extension at 72˚C for 7 min. The ScFv fragment was then linked into pAdTrack-CMV (plasmid no. 16405; Addgene, Inc., Cambridge, MA, USA), a shuttle adenoviral plasmid (pAd). The recombinant pAdTrack-ScFv shuttle plasmid was identified by PCR, *Kpn*I and *Hin*dIII enzyme (Takara Biotechnology Co., Ltd.) restriction digestion and sequencing.

Construction and packaging of recombinant adenoviral vector pAd-ScFv. *Pme*I enzyme (New England BioLabs, Inc., Ipswich, MA, USA) was used to linearly cut pAdTrack-ScFv shuttle plasmid. After purification, it was transformed into competent BJ5183 bacteria with pAdEasy-1 (both from Agilent Technologies, Inc., Santa Clara, CA, USA) for homogenous recombination. After recovery at 37˚C for 1 h, bacteria were cultured on a plate with kanamycin and ampicillin. The positive clone was collected for identifying correctly constructed recombinant pAd-ScFv by PCR and *Pac*I enzyme (New England BioLabs, Inc.) restriction digestion.

A total of $5x10^6$/ml HEK293 cells (Cell Bank, Chinese Academy of Sciences, Shanghai, China) were seeded in culture flasks. When the cell density reached 60-70%, pAd-ScFv plasmid linearly cut by *Pac*I endonuclease restriction enzyme was transfected into the cells by using Lipofectamine 2000 (Thermo Fisher Scientific, Inc.). After 24 h, the fluorescence in the cells was observed. When 1/3-1/2 of the cells became round and floated, cells were collected, centrifuged and re-suspended. Virus-containing supernatant was obtained by using the Adenovirus Purification and Concentration kit (Merck KGaA, Darmstadt, Germany). Recurrent infection into HEK293 cells was then performed to obtain a large amount of pAd-ScFv recombinant adenovirus.

Viral transfection. H9C2 cells (Cell Bank, Chinese Academy of Sciences) were cultured in Dulbecco's modified Eagle's medium with 10% fetal bovine serum (Thermo Fisher Scientific, Inc.). Cells ($2x10^5$/ml) were seeded into a 6-well plate at 2.5 ml/well and cultured for 2 h at 37˚C in a humidified atmosphere containing 5% CO_2. The recombinant pAd-ScFv was transfected into H9C2 cells (pAd-ScFv infection group). An empty vector infection group and blank control group were also set up. After transfection for 48 h, cells were collected.

Western blot analysis. Western blot analysis was used to detect the expression of N-cadherin and C-terminal fragment of N-cadherin (CTF1). In brief, proteins were extracted from transfected cells and heart tissues using lysis buffer (Beyotime Institute of Biotechnology, Haimen, China). The protein concentration was determined using the BCA protein assay kit (P0012A; Beyotime Institute of Biotechnology). Protein (30-50 μg per lane) was separated by 12% SDS-PAGE and transferred onto polyvinylidene difluoride membranes. After washing and blocking with bovine serum albumin (BSA) (Sigma-Aldrich; Merck KGaA, Darmstadt, Germany) for 1 h, primary rabbit anti-human polyclonal anti-N-cadherin antibody (ab18203; 1:1,000; Abcam, Cambridge, MA, USA) was added, followed by incubation overnight at 4˚C. The primary

antibody for N-cadherin also recognizes antigenic epitopes of CTF1, so the antibody for CTF1 was the same as the antibody for N-cadherin. After washing the membrane, a secondary horseradish peroxidase (HRP)-labeled goat anti-rabbit antibody (sc-2004, 1:1,000; Santa Cruz Biotechnology, Inc., Dallas, TX, USA) was added, followed by incubation for 1 h at room temperature. The membrane was then developed using enhanced chemiluminescence plus reagent (PerkinElmer, Inc., Waltham, MA, USA). β-actin was detected by anti-β-actin antibody (sc-69879, 1:1,000; Santa Cruz Biotechnology, Inc.), which was used as an internal reference. Each sample was analyzed in three replicates. Detection of HRP was performed by Chemiluminescent Imaging and Analysis system (Beijing Sage Creation Science Co., Ltd., Beijing, China).

Flow cytometric analysis. After digestion with trypsin, pAd-ScFv-infected H9C2 cells were collected and washed in PBS with centrifugation at 200 x g at 4˚C for 3 min. Cells were stained with fluorescence-labeled anti-N-cadherin antibody (ab195185, 1:1,000 dilution; Abcam) in PBS for 30 min at 4˚C, while cells in the control group were treated with PBS only. After washing with PBS twice, the cells were re-suspended in PBS at 4˚C and immediately subjected to flow cytometric analysis (BD FACSCalibur, BD Biosciences, Franklin Lakes, NJ, USA). The average fluorescence of 50,000 cells was used to determine the expression levels of N-cadherin.

Cell adhesion assay. Fibronectin (10 μg/ml, 100 μl per well, Merck KGaA) was used to coat 96-well plates. Wells coated with 1% BSA and 100 μg/ml poly-lysine were used as reference for minimum and maximum adhesion, respectively. Cell suspension ($5x10^5$ cells/ml; 100 μl) from the pAd-ScFv infection group, mock infection group or blank control group was added, followed by incubation for 3 h at 37˚C. PBS was used to rinse off non-adherent cells. Cells were then fixed with paraformaldehyde and stained with 1% methylene blue for 20 min. Subsequently, 100 μl HCl (1 mol/l) was added, followed by incubation at 37˚C for 40 min. The absorbance (A) at 600 nm was detected by using a microplate reader. The cell adhesion rate was calculated by using the following formula: $(A_{\text{test group}} - A_{\text{BSA well}})/(A_{\text{poly-lysine well}} - A_{\text{BSA well}}) \times 100\%$.

Animal grouping and treatment. A rat model of DCM was established by intraperitoneal injection of 2 ml/kg adriamycin (Merck KGaA) once a week for 6 weeks. Adult male Sprague-Dawley rats (purchased from the Experimental Animal Center of Wuhan University, Wuhan, China) were divided into 4 groups: Normal control group (n=10), DCM model group (n=25), ScFv treatment group (n=25) and empty vector control group (n=25). Two or three rats were housed per cage under specific pathogen-free conditions (controlled temperature of 24±3˚C and humidity of 55±15%) with a 12-h light/dark cycle and *ad libitum* access to food and tap water. In the normal control group, intravenous injection with the same volume of saline once a week for 8 weeks was performed. In the DCM model group, rats received intraperitoneal injection of 2 ml/kg adriamycin once a week for 6 weeks. In the ScFv treatment group, at the end of the 6-week adriamycin treatment, 30 μl pAd-ScFv at 10^{10} pfu/ml was injected into 6 sites on the right ventricle diaphragmatic surface of DCM rats after exposing the heart (21). In the empty vector treatment group, an equal volume of empty vector was injected into the DCM rats. At 72 h after injection, 3 rats from the pAd-ScFv transfection group were used to isolate primary myocardial cells and detect fluorescence. Rats in the other groups and the remaining rats in the transfection group were used for examination of heart function by ultrasonography. Subsequently, rats were sacrificed to collect specimens for the other analyses. This study was carried out in strict accordance with international, national and institutional rules regarding animal experiments and all surgery was performed under sodium pentobarbital anesthesia. All efforts were made to minimize suffering. The protocol was approved by the Committee on the Ethics of Animal Experiments of the Wuhan University (permit no. WDRY2013-L016).

Measurement of heart function. Rats in each group were anesthetized by intraperitoneal injection of 10% chloral hydrate (3 ml/kg; Sigma-Aldrich; Merck KGaA). Cardiac color Doppler ultrasound VIVID7 (GE Healthcare, Little Chalfont, UK) with a 12-MHz probe was used to detect the heart chamber diameter and cardiac function. The left ventricular end diastole (LVED), left ventricular end systole (LVES), fraction shortening (FS), left ventricular ejection fraction (LVEF) and interventricular septal thickness (IVS) were recorded.

Hematoxylin and eosin (H&E) staining. Ventricular myocardium of rats in each group was collected and fixed with 4% paraformaldehyde. The tissue was paraffin-embedded and sliced for H&E staining. The stained tissues were observed under a microscope and images were captured.

Immunohistochemistry. Paraffin-embedded tissues were serially sectioned and the routine streptavidine-avidine-biotin complex method was used for immunohistochemistry based on the standard protocol of the SABC-kit (SP-9000, Beijing Zhongshan Jinqiao Biotechnology Co., Ltd., Beijing, China). The primary polyclonal antibody for N-cadherin was same as that used for western blot analysis (dilution, 1:150; 4˚C; overnight). Samples were further processed using a Goat anti-rabbit IgG IHC kit (PV-9001, Beijing Zhongshan Jinqiao Biotechnology Co., Ltd.), and the sections were counterstained with hematoxylin. In the negative control, PBS was used to replace the primary antibody. Cells with brown staining or granules in the cytoplasm or nucleus were defined as expressing N-cadherin. Ten fields of view were randomly selected under high magnification (x200). Cells with N-cadherin staining were counted and their percentage was determined. The average percentage was used as the relative protein expression levels in myocardial cells. The same brown was used as a standard to estimate the relative expression for each section and analyze the integrated optical density values (IOD). The average IOD of the images for each group was represented as the mean ± standard deviation (SD).

Statistical analysis. SPSS 11.0 software (SPSS, Inc., Chicago, IL, USA) was used for statistical analysis. Values are expressed as the mean ± SD. If there was homogeneity of variance, a paired Student's t-test was used. If there was heterogeneity, differences among groups were determined by analysis of

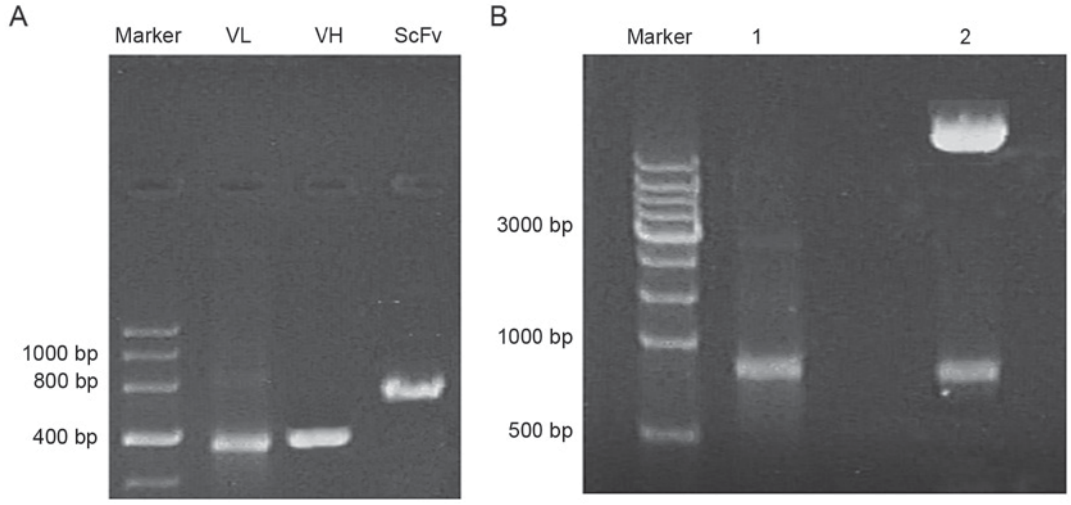

Figure 1. Construction of pAdTrack-ScFv adenoviral shuttle plasmid. (A) Clone of V_H, V_L and ScFv gene. (B) Enzyme and PCR analysis of pAdTrack-ScFv (lanes: 1, PCR product of pAdTrack-ScFv; 2, enzyme-digested products of pAdTrack-ScFv). PCR, polymerase chain reaction; pAd, adenoviral plasmid; ScFv, single chain variable fragment; V_H, heavy chain variable domain; V_L, light chain variable domain.

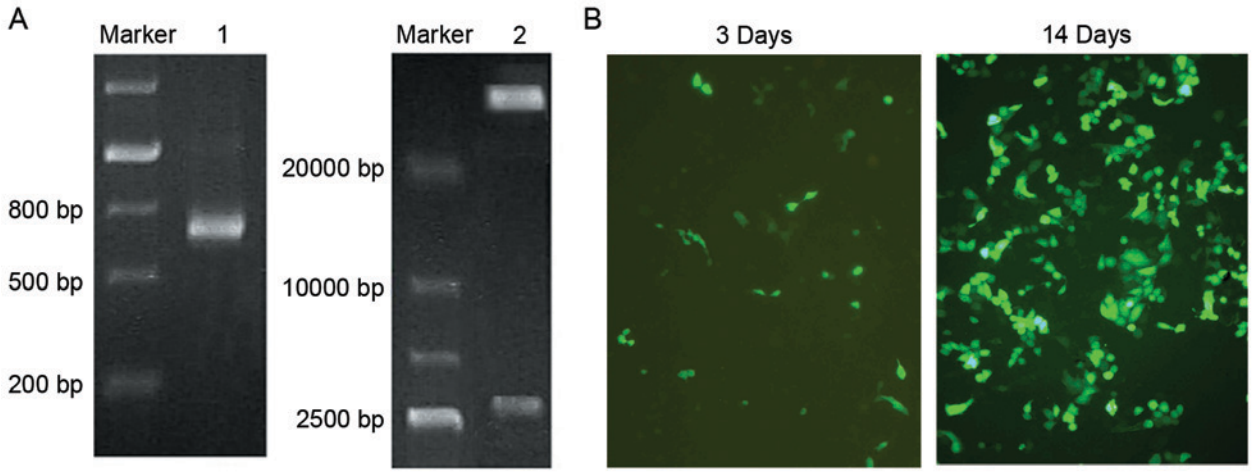

Figure 2. Construction and packaging of recombinant pAd-ScFv plasmid. (A) PCR product of pAd-ScFv and product digested by *Pac*I enzyme (lanes: 1, PCR product of recombinant pAd-ScFv adenovirus; 2, *Pac*I enzyme-digested products of recombinant pAd-ScFv. (B) Fluorescence in HEK293 cells after transfection with pAd-ScFv expressing enhanced green fluorescent protein after 3 and 14 days. Magnification, x200. PCR, polymerase chain reaction; pAd-ScFv, single chain variable fragment adenoviral plasmid.

variance. P<0.05 was considered to indicate a statistically significant difference.

Results

Construction of pAdTrack-ScFv adenoviral shuttle plasmid and recombinant adenoviral pAd-ScFv. To obtain the ScFv fragment, the V_{H1} (410 bp) and V_{L1} (380 bp) templates were first amplified in the 2B3 cell line to secrete monoclonal antibody recognizing a sequence of N-cadherin containing the ADAM10 hydrolysis site. SOE-PCR was used to obtain the ScFv fragment of ~750 bp in length, which was identified by gel electrophoresis (Fig. 1A). As presented in Fig. 1B, the full-length ScFv gene was inserted into the adenoviral shuttle plasmid pAdTrack-CMV to construct pAdTrack-ScFv. After linearization by digestion with *Pme*I, pAdTrack-ScFv adenoviral shuttle plasmid was homologously recombined with a pAdEasy-1 backbone vector. Following identification by PCR, the specific band of a nucleotide with the length of 750 bp was amplified (Fig. 2A). The adenoviral plasmid was then digested by *Pac*I and electrophoretic analysis was used for further confirmation (Fig. 2A).

The Lipofectamine method was used for transfecting pAd-ScFv into HEK293 cells. After 72 h, fluorescence was observed in the HEK293 cells, which gradually increased when the culture time was extended. After 14 days of transfection, the cells became enlarged and formed clusters (Fig. 2B). These cells were used to obtain recombinant pAd-ScFv adenovirus.

pAd-ScFv increases N-cadherin and decreases CTF1 protein levels in cardiomyocytes. To detect the levels of N-cadherin and CTF1 protein in H9C2 cells after transfection, western blot analysis was used. As presented in Fig. 3A, N-cadherin protein levels were significantly increased in the transfection group compared with those in the blank control group, while CTF1 protein levels were significantly decreased. The results

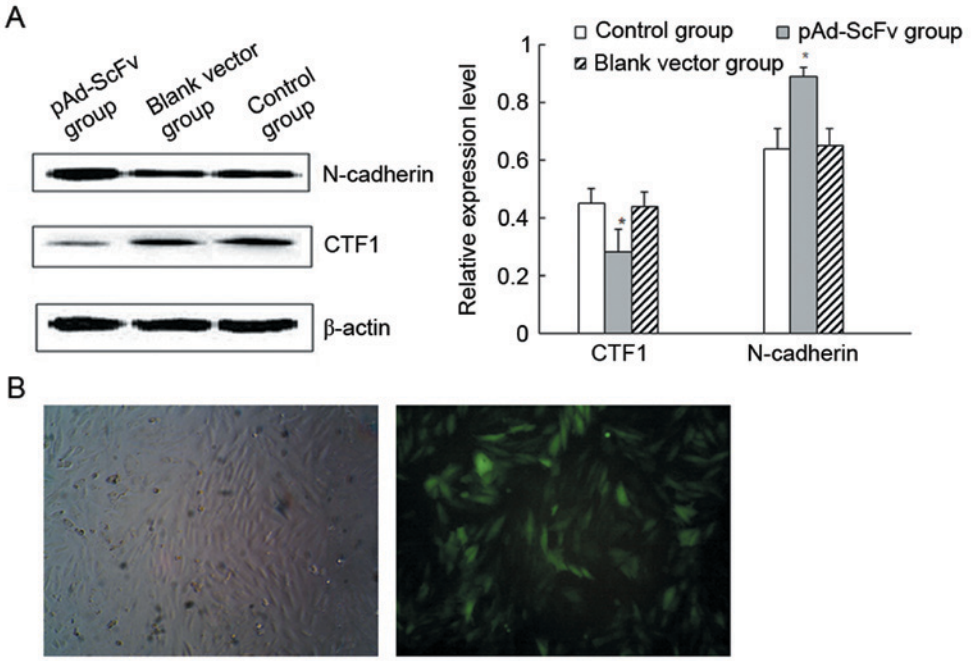

Figure 3. Changes of N-cadherin and CTF1 levels in H9C2 cells after transfection with recombinant pAd-ScFv adenovirus. (A) Compared with the blank group, N-cadherin protein was significantly increased in H9C2 cells after transfection with recombinant pAd-ScFv, while CTF1 expression was significantly decreased; *P<0.05 vs. control group. (B) Fluorescence was observed in H9C2 cells after transfection with recombinant pAd-ScFv expressing enhanced green fluorescent protein. Magnification, x100. CTF1, C-terminal fragment 1 of N-cadherin; pAd-ScFv, single chain variable fragment adenoviral plasmid.

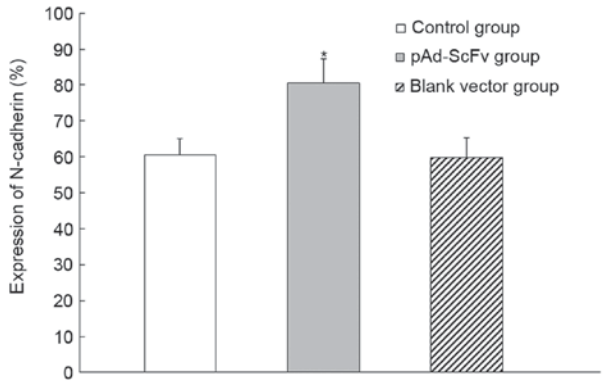

Figure 4. Detection of N-cadherin on the surface of H9C2 cells by flow cytometry. N-cadherin was significantly increased in the pAd-ScFv group compared with that in the control group. *P<0.05 vs. control group. pAd-ScFv, single chain variable fragment adenoviral plasmid.

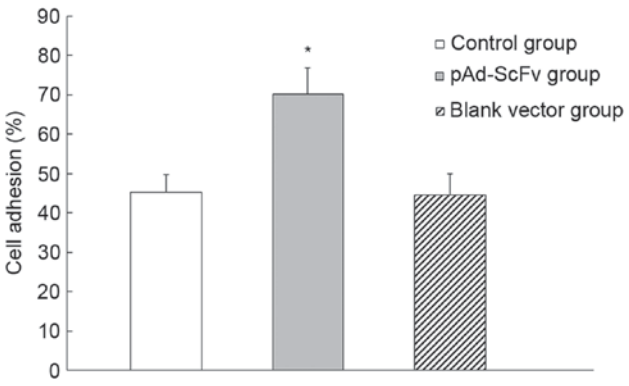

Figure 5. Changes of the cell adhesive ability of H9C2 cells. The cell adhesion capability was significantly promoted in pAd-ScFv group compared with that in the control group. pAd-ScFv, single chain variable fragment adenoviral plasmid.

indicated that transfection of the recombinant adenoviral vector decreased CTF1 and increased N-cadherin protein levels. As demonstrated in Fig. 3B, pAd-ScFv was successfully transfected into H9C2 cells.

pAd-ScFv increases N-cadherin on the surface of myocardial cells in vitro. To detect the changes of N-cadherin protein on the surface of myocardial cells, flow cytometry was used. As presented in Fig. 4, N-cadherin protein on the myocardial cell surface was significantly increased in the pAd-ScFv infection group compared with that in the control groups (P<0.05). These results indicated that pAd-ScFv decreased the hydrolysis process on N-cadherin by ADAM10 through blocking the ADAM10 hydrolysis site in N-cadherin.

pAd-ScFv increases myocardial cell adhesion. The influence of pAd-ScFv on the adhesion of H9C2 cells was assessed. As presented in Fig. 5, the cell adhesion rate in the pAd-ScFv group was 70.23±6.5%, while it was 45.21±4.5% in the blank group and 44.58±5.7% in the empty plasmid group. The pAd-ScFv group had a significantly higher adhesion rate compared with that in the control groups (P<0.05), which indicated that pAd-ScFv increased the adhesion capability of myocardial cells.

Fluorescence detection of pAd-ScFv in primary myocardial cells of rats in the transfection group. To confirm that transfection was successful, the fluorescence in primary myocardial cells isolated from rats in the transfection group was detected. As presented in Fig. 6, a large amount of fluorescence was

Table I. Parameters of heart function in the experimental groups of rats.

Group	LVED (mm)	LVES (mm)	IVS (mm)	LVEF (%)	FS (%)
Normal control	5.62±0.45	2.83±0.36	1.95±0.32	92±2	58±4
Model	6.73±0.52[a]	4.05±0.22[a]	3.05±0.43[a]	80±5[a]	44±3[a]
pAd-ScFv treatment	5.82±0.33[b]	3.28±0.40[b]	2.03±0.24[b]	88±6[b]	55±2[b]
Empty vector control	6.65±0.42[a]	4.03±0.54[a]	2.98±0.42[a]	81±4[a]	46±3[a]

[a]P<0.01 compared with normal control group; [b]P<0.01 compared with model group. Values are expressed as the mean ± standard deviation. LVED, left ventricular end diastole; LVES, left ventricular end systole; FS, fraction shortening; LVEF, left ventricular ejection fraction; IVS, interventricular septal thickness; pAd-ScFv, single chain variable fragment adenoviral plasmid.

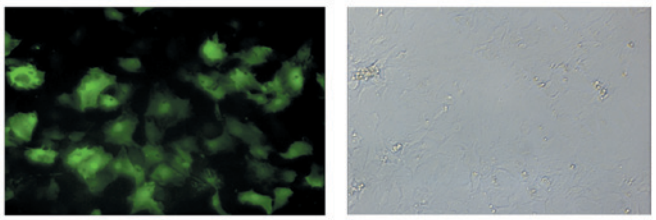

Figure 6. Fluorescence observed in primary cardiac cells isolated from the hearts of rats with dilated cardiomyopathy at 72 h after injection of single chain variable fragment adenoviral plasmid expressing enhanced green fluorescence protein. Magnification, x200.

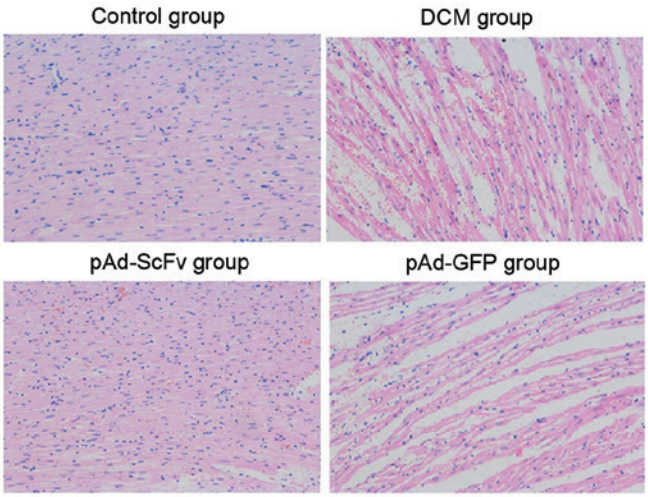

Figure 7. Hematoxylin and eosin-stained myocardial tissues of rats from each experimental group, demonstrating morphological and pathological changes. Magnification, x200. DCM, dilated cardiomyopathy; GFP, green fluorescent protein; pAd-ScFv, single chain variable fragment adenoviral plasmid.

observed in isolated primary myocardial cells, which indicated that the transfection of the rat model was successful.

pAd-ScFv improves heart function in a rat model of DCM. In the DCM model group, a total of 10 rats had died (mortality rate, 40%), the main reason of which was congestive heart failure. In the treatment group, the mortality rate was 12%, which was significantly lower than that in the model group (P<0.01), while it was 36% in the empty vector group (P>0.05 vs. model group). In the blank normal control group, none of the rats

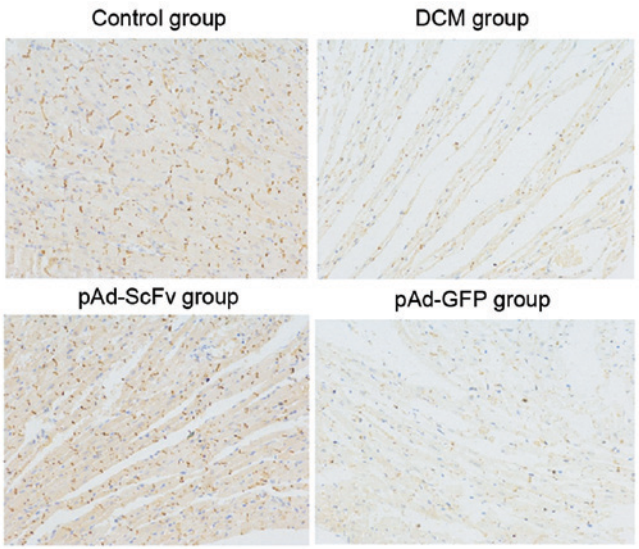

Figure 8. N-cadherin on the surface of myocardial cells of each group of rats. Magnification, x200. DCM, dilated cardiomyopathy; GFP, green fluorescent protein; pAd-ScFv, single chain variable fragment adenoviral plasmid.

died. The heart function was compared between the different groups (Table I). Compared with those in the control group, the LVED, LVES and IVS were significantly increased in the DCM model group, while the LVEF and FS were significantly decreased. In the pAd-ScFv treatment group, the myocardial structure and heart function were significantly improved. Compared with those in the model group, the LVED, LVES and IVS were significantly decreased, while LVEF and FS were increased.

pAd-ScFv reduces DCM-induced pathological changes in rat myocardial tissues. To explore the pathological changes of myocardial tissues among different groups, H&E staining was performed. As demonstrated in Fig. 7, a normal morphology of cardiomyocytes was observed in the normal control group and the cytoplasm was clear. In the model group and the empty vector control group, necrosis was observed. Cardiomyocytes were enlarged with widened gaps. Myocardial fibers were fractured, and hyperplasia of endocardial collagen and elastic fibers was observed. Certain parts of myocardial tissues had been replaced by fibrous tissues and certain areas of the cardiac sarcoplasm were condensed. Cell nuclei were condensed, distorted or had disappeared, and fat was degenerated.

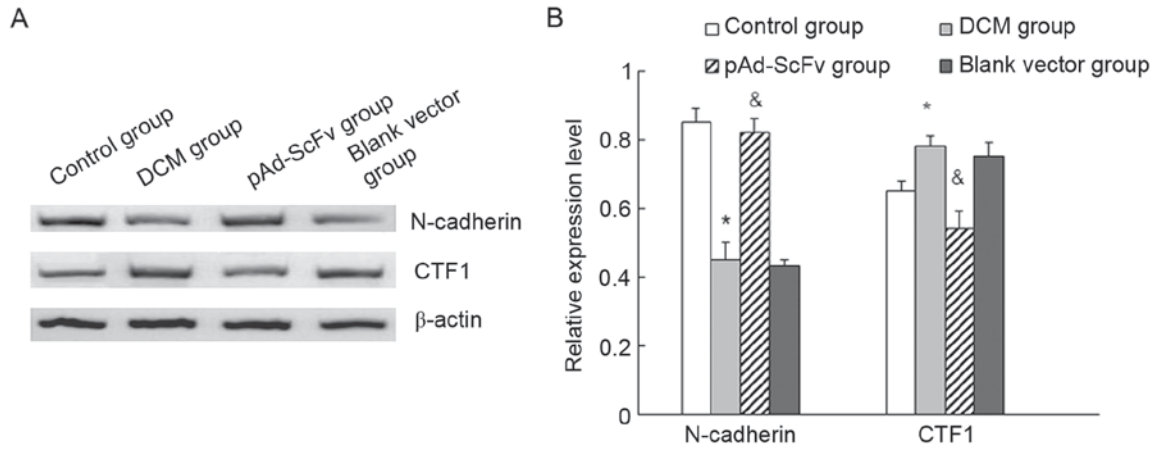

Figure 9. Levels of N-cadherin and CTF1 in myocardial tissues of each group of rats. (A) Representative western blot images for the expression of N-cadherin and CTF1. (B) Quantitative evaluation of western blots demonstrated that compared with the control group, N-cadherin protein was significantly decreased in the DCM group (P<0.05), while it was significantly increased in the pAd-ScFv group compared with that in the DCM group (P<0.05). The opposite trend was seen for CTF1. *P<0.05 vs. control group, &P<0.05 vs. DCM group. DCM, dilated cardiomyopathy; CTF1, C-terminal fragment 1 of N-cadherin; pAd-ScFv, single chain variable fragment adenoviral plasmid.

Table II. Expression of N-cadherin in the myocardial cells of different groups.

Group	Integrated optical density
Normal control	4129.73±1154.72
Model	1073.55±509.44[a]
pAd-ScFv treatment	3664.50±1713.91[b]
Empty vector control	1127.25±679.87[b]

[a]P<0.01 compared with normal control group; [b]P<0.01 compared with model group. Values are expressed as the mean ± standard deviation. pAd-ScFv, single chain variable fragment adenoviral plasmid.

Cytoplasmic vacuolization in cells, lymphocyte infiltration, fibroblast proliferation and capillary hyperplasia were also observed. In the pAd-ScFv treatment group, all of the above pathological changes were obviously improved.

pAd-ScFv increases N-cadherin on the surface of myocardial cells of DCM model rats. To assess the effect of pAd-ScFv on N-cadherin on the surface of myocardial cells of DCM rats, immunohistochemical staining was performed. As presented in Fig. 8 and Table II, N-cadherin was obviously decreased in the model group compared with that in the normal control group. In the pAd-ScFv treatment group, N-cadherin was increased, as ScFv blocked the ADAM10 hydrolysis site in N-cadherin.

pAd-ScFv increases N-cadherin and decreases CTF1 in the myocardial tissues of DCM rats. The levels of N-cadherin and CTF1 in heart tissues of the different groups of rats were assessed by western blot analysis. As displayed in Fig. 9, N-cadherin protein levels were significantly decreased in the model group compared with those in the control group, while they were significantly increased in the treatment group compared with those in the model group. Furthermore, CTF1 protein was significantly increased in the model group compared with that in the control group, while it was significantly decreased in the transfection group compared with that in the model group.

Discussion

DCM is characterized by left ventricle or dysfunction of the left and right ventricular dilatation and systole, which is a disease representative of chronic congestive heart failure. A previous study reported that ventricular remodeling is important in cardiac dysfunction (22). Ventricular remodeling includes mechanical and electrical remodeling. Changes in the number of connections of intercalated discs to cardiac cells as well as their distribution and functional disorders have important roles in processes of ventricular mechanical remodeling (23). N-cadherin-mediated connections are essential for cardiomyocyte adhesion. N-cadherin combines with catenin to form the cadherin-catenin complex, which is an important structure in maintaining myocardial morphology, substance transport and trans-membrane signal transfer (24). Studies have demonstrated that abnormal structure and function of the cadherin-catenin complex are closely associated with ventricular remodeling (25). ADAMs have important roles in processing N-cadherin in fibroblast cells and nerve cells (16), thereby regulating the cellular distribution of N-cadherin and the formation of the cadherin-catenin complex. ADAM10, one member of the family of ADAMs, has the most critical role in the proteolytic processing of N-cadherin. ADAM10 hydrolyzes the N-terminal R714-I715 site in the extracellular domain of N-cadherin, thus producing CTF1 and NTF fragments. The integrity of N-cadherin molecules is destroyed, which further affects the formation of the cadherin-catenin complex. Previous studies by our group found that this hydrolysis pathway for processing N-cadherin was present in cardiomyocytes (19,26). Current research focuses on the interaction of ADAMs and N-cadherin in cardiomyocytes and their participation in processes of ventricular remodeling, with a specific focus on ADAM10 inhibitors, including

RNA interference and antibody-mediated blocking. However, direct inhibition of ADAM10 has certain flaws and shortcomings: Besides N-cadherin, ADAM10 has numerous other substrates, which have important roles in normal physiological processes, and therefore, inhibition of the activity of ADAM10 has severe side effects, including changes of cell adhesion, chemokine function, immune disorders and developmental defects of the nervous and cardiovascular systems (27,28).

In the present study, ScFv antibody was used to block the ADAM10 hydrolysis site in N-cadherin. This strategy has two advantages: First, it specially interferes with the interaction of N-cadherin with ADAM10 and does not affect the hydrolysis of any of the other substrates of ADAM10, thereby avoiding effects not specific for N-cadherin processing. Furthermore, N-cadherin prefers to form the cadherin-catenin complex to exert its physiological functions in response to blocking of the hydrolysis site. To pursue this strategy, the recombinant adenoviral pAd-ScFv vector was constructed. After transfection into H9C2 cells, the protein levels of N-cadherin were significantly increased, while CTF1 was significantly decreased. Flow cytometric analysis demonstrated that N-cadherin on the cell surface was significantly increased in transfected myocardial cells compared with that in the control group, which indicated that ADAM10 had important roles in the hydrolysis of N-cadherin in myocardial cells. A cell adhesion assay indicated that the adhesion ability of myocardial cells was significantly increased by the antibody. The results further indicated that N-cadherin hydrolysis by ADAM10 destroyed the integrity of N-cadherin and influenced the formation of the cadherin-catenin complex, which induced associated pathological and physiological changes.

In addition to the *in vitro* cell-based experiments, the recombinant pAd-ScFv adenovirus was also injected into the hearts of rats with adriamycin-induced DCM. Compared with that in the model group, the structure and function of the heart was significantly improved in the ScFv treatment group. Western blot analysis indicated that N-cadherin protein was significantly increased in the ScFv treatment group and that CTF1 protein was significantly reduced compared with that in the control group. Immunohistochemical analysis revealed that N-cadherin protein on the myocardial cell surface was significantly increased by pAd-ScFv. These results indicated that N-cadherin was increased by ScFv through blocking the ADAM hydrolysis site on N-cadherin, which promoted the formation of the cadherin-catenin complex, thereby enhancing cardiomyocyte adhesion to inhibit myocardial remodeling and delay heart failure.

In conclusion, pAd-ScFv adenovirual plasmid was successfully constructed and transfected into cardiomyocytes. The ADAM10 hydrolysis site in N-cadherin was specifically blocked, leading to high levels of N-cadherin. Intracardial injection of pAd-ScFv was found to ameliorate DCM in rats. The present findings broadened the current understanding of the pathogenesis of DCM; it was indicated that the degradation of N-cadherin by highly expressed ADAM10 in cardiomyocytes is one of the reasons for ventricular remodeling in DCM. The results of the present study may also provide an experimental foundation for the prevention and treatment of DCM.

Acknowledgements

The present study was supported by the National Natural Science Foundation of China (no. 8100094), the Natural Science Foundation of Hubei Province (no. 2012FFB04418) and the Wuhan Health and Family Planning Commission Project (no. WX14C71).

References

1. Ye XZ, Zhi H, Cao K, Li J, Li XL, Gu K, Zhang HF, Xu F, Zhou YL, Zhou L and Xu DJ: A research about the relationship between cardiac and renal function in dilated cardiomyopathy patients with heart failure. Lin Chuang Xin Xue Guan Bing Za Zhi 26: 104-108, 2010 (In Chinese).
2. Konstam MA, Kramer DG, Patel AR, Maron MS and Udelson JE: Left ventricular remodeling in heart failure: Current concepts in clinical significance and assessment. JACC Cardiovasc Imaging 4: 98-108, 2011.
3. Ruiz-Zamora I, Rodriguez-Capitan J, Guerrero-Molina A, Morcillo-Hidalgo L, Rodriguez-Bailon I, Gomez-Doblas JJ, de Teresa-Galvan E and Garcia-Pinilla JM: Incidence and prognosis implications of long term left ventricular reverse remodeling in patients with dilated cardiomyopathy. Int J Cardiol 203: 1114-1121, 2016.
4. Yoon JH, Son JW, Chung H, Park CH, Kim YJ, Chang HJ, Hong GR, Kim TH, Ha JW, Choi BW, *et al*: Relationship between myocardial extracellular space expansion estimated with post-contrast T1 mapping MRI and left ventricular remodeling and neurohormonal activation in patients with dilated cardiomyopathy. Korean J Radiol 16: 1153-1162, 2015.
5. Huang J, Ni XD, Hu YP, Song ZW, Yang WY and Xu R: Left ventricular longitudinal rotation changes in patients with dilated cardiomyopathy detected by two-dimensional speckle tracking imaging. Zhonghua Xin Xue Guan Bing Za Zhi 39: 920-924, 2011 (In Chinese).
6. Pahl E, Sleeper LA, Canter CE, Hsu DT, Lu M, Webber SA, Colan SD, Kantor PF, Everitt MD, Towbin JA, *et al*: Incidence of and risk factors for sudden cardiac death in children with dilated cardiomyopathy: A report from the pediatric cardiomyopathy registry. J Am Coll Cardiol 59: 607-615, 2012.
7. Ram R, Wescott AP, Varandas K, Dirksen RT and Blaxall BC: Mena associates with Rac1 and modulates connexin 43 remodeling in cardiomyocytes. Am J Physiol Heart Circ Physiol 306: H154-H159, 2014.
8. Hertig CM, Butz S, Koch S, Eppenberger-Eberhardt M, Kemler R and Eppenberger HM: N-cadherin in adult rat cardiomyocytes in culture. II. Spatio-temporal appearance of proteins involved in cell-cell contact and communication. Formation of two distinct N-cadherin/catenin complexes. J Cell Sci 109: 11-20, 1996.
9. Frank D, Rangrez AY, Poyanmehr R, Seeger TS, Kuhn C, Eden M, Stiebeling K, Bernt A, Grund C, Franke WW and Frey N: Mice with cardiac-restricted overexpression of Myozap are sensitized to biomechanical stress and develop a protein-aggregate-associated cardiomyopathy. J Mol Cell Cardiol 72: 196-207, 2014.
10. Chen SN, Gurha P, Lombardi R, Ruggiero A, Willerson JT and Marian AJ: The hippo pathway is activated and is a causal mechanism for adipogenesis in arrhythmogenic cardiomyopathy. Circ Res 114: 454-468, 2014.
11. Asimaki A, Kapoor S, Plovie E, Karin Arndt A, Adams E, Liu Z, James CA, Judge DP, Calkins H, Churko J, *et al*: Identification of a new modulator of the intercalated disc in a zebrafish model of arrhythmogenic cardiomyopathy. Sci Transl Med 6: 240ra74, 2014.
12. Zhou J, Qu J, Yi XP, Graber K, Huber L, Wang X, Gerdes AM and Li F: Up-regulation of gamma-catenin compensates for the loss of beta-catenin in adult cardiac myocytes. Am J Physiol Heart Circ Physiol 292: H270-H276, 2007.
13. Sodian R, Hoerstrup SP, Sperling JS, Daebritz S, Martin DP, Moran AM, Kim BS, Schoen FJ, Vacanti JP and Mayer JE Jr: Early in vivo experience with tissue-enginered trileaflet heart valves. Circulation 102 (19 Suppl 3): III22-III29, 2000.
14. Jannesari-Ladani F, Hossein G, Monhasery N, Shahoei SH and Izadi Mood N: Wnt5a influences viability, migration, adhesion, colony formation, E- and N-cadherin expression of human ovarian cancer cell line SKOV-3. Folia Biol (Praha) 60: 57-67, 2014.

15. Vega L JC, Lee MK, Jeong JH, Smith CE, Lee KY, Chung HJ, Leckband DE and Kong H: Recapitulating cell-cell adhesion using N-cadherin biologically tethered to substrates. Biomacromolecules 15: 2172-2179, 2014.
16. Reiss K, Maretzky T, Ludwig A, Tousseyn T, de Strooper B, Hartmann D and Saftig P: ADAM10 cleavage of N-cadherin and regulation of cell-cell adhesion and beta-catenin nuclear signaling. EMBO J 24: 742-752, 2005.
17. Matsuda T, Fujio Y, Nariai T, Ito T, Yamane M, Takatani T, Takahashi K and Azuma J: N-cadherin signals through Rac1 determine the localization of connexin 43 in cardiac myocytes. J Mol Cell Cardiol 40: 495-502, 2006.
18. Uemura K, Kihara T, Kuzuya A, Okawa K, Nishimoto T, Ninomiya H, Sugimoto H, Kinoshita A and Shimohama S: Characterization of sequential N-cadherin cleavage by ADAM10 and PS1. Neurosci Lett 402: 278-283, 2006.
19. Li XO, Huang W, Chen YJ and Zhou LR: Silencing of ADAM10 gene by siRNA inhibits the ADAMs cleavage of N-cadherin in cardiac myocytes. Zhongguo Bing Li Sheng Li Za Zhi 9: 1702-1704, 2012 (In Chinese).
20. Fedak PW, Moravec CS, McCarthy PM, Altamentova SM, Wong AP, Skrtic M, Verma S, Weisel RD and Li RK: Altered expression of disintegrin metalloproteinases and their inhibitor in human dilated cardiomyopathy. Circulation 113: 238-245, 2006.
21. Toivonen R, Koskenvuo J, Merentie M, Söderström M, Ylä-Herttuala S and Savontaus M: Intracardiac injection of a capsid-modified Ad5/35 results in decreased he-art toxicity when compared to standard Ad5. Virol J 9: 296, 2012.
22. Zhang YJ, Yang SH, Li MH, Iqbal J, Bourantas CV, Mi QY, Yu YH, Li JJ, Zhao SL, Tian NL and Chen SL: Berberine attenuates adverse left ventricular remodeling and cardiac dysfunction after acute myocardial infarction in rats: Role of autophagy. Clin Exp Pharmacol Physiol 41: 995-1002, 2014.
23. Severs NJ, Dupont E, Thomas N, Kaba R, Rothery S, Jain R, Sharpey K and Fry CH: Alterations in cardiac connexin expression in cardiomyopathies. Adv Cardiol 42: 228-242, 2006.
24. Severs NJ, Coppen SR, Dupont E, Yeh HI, Ko YS and Matsushita T: Gap junction alterations in human cardiac disease. Cardiovasc Res 62: 368-377, 2004.
25. Yang Z, Bowles NE, Scherer SE, Taylor MD, Kearney DL, Ge S, Nadvoretskiy VV, DeFreitas G, Carabello B, Brandon LI, *et al*: Desmosomal dysfunction due to mutations in desmoplakin causes arrhythmogenic right ventricular dysplasia/cardiomyopathy. Circ Res 99: 646-655, 2006.
26. Li XO, Huang W and Zhou LR: Construction of lentiviral vector of RNA interference of ADAM10 gene and its inhibitive role on the ADAMs cleavage of N-cadherin in cardiac myocyte. Guo Ji Mian Yi Xue Za Zhi 36: 221-225, 2013 (In Chinese).
27. Jakobsson L, Franco CA, Bentley K, Collins RT, Ponsioen B, Aspalter IM, Rosewell I, Busse M, Thurston G, Medvinsky A, *et al*: Endothelial cells dynamically compete for the tip cell position during angiogenic sprouting. Nat Cell Biol 12: 943-532, 2010.
28. Liu H, Zhang W, Kennard S, Caldwell RB and Lilly B: Notch3 is critical for proper angiogenesis and mural cell investment. Circ Res 107: 860-870, 2010.